DYNAMICAL HYSTERESIS

paper1

Critical slowing down at a bifurcation

J. R. Tredicce and G. L. Lippi[a)]
Institut Non Linéaire de Nice, UMR 6618 CNRS–UNSA, 1361 Route des Lucioles, F-06560 Valbonne, France

Paul Mandel
Optique Nonlinéaire Théorique, Campus Plaine CP 231, Université Libre de Bruxelles, 1050 Bruxelles, Belgium

B. Charasse,[b)] A. Chevalier,[b)] and B. Picqué[b)]
Département de Physique, Université de Nice-Sophia Antipolis, Parc Valrose, F-06108 Nice, Cedex, France

(Received 10 June 2002; accepted 2 February 2004)

Critical slowing down near a bifurcation or limit point leads to a dynamical hysteresis that cannot be avoided by sweeping a control parameter slowly through the critical point. This paper analytically illustrates, with the help of a simple model, the bifurcation shift. We describe an inexpensive experiment using a semiconductor laser where this phenomenon occurs near the threshold of a semiconductor laser. © *2004 American Association of Physics Teachers.*
[DOI: 10.1119/1.1688783]

I. INTRODUCTION

The study of bifurcations has gained considerable attention in recent decades due to the role that they play in the characterization of the behavior of nonlinear systems. The transition from one state to another is accompanied by the exchange of stability (or at least by a modification of the basin of attraction) of coexisting solutions. Such a change of state can in many instances be characterized by simple, generic equations, whose topological properties closely describe the system's states and the transitions between them. Bifurcations are reported in varied nonlinear systems, from mechanical systems[1] (for example, magnetostrictive ribbons, a spinning top, and a bouncing ball), to spin waves in ferromagnetic materials,[2] chemical[3] and hydrodynamical systems,[4] and lasers.[5] A good introduction to bifurcations can be found in Ref. 6.

In this paper we highlight a counterintuitive property of bifurcations. Suppose that by varying a control parameter μ such as the temperature, a driving electric current, or a chemical concentration, we find a phase transition such that one phase is stable if $\mu<\mu_c$ and the other phase is stable if $\mu>\mu_c$. This behavior is static, obtained by choosing a value of μ, letting the system relax to its final state, and repeating the procedure for each value of μ. However, it often is practical or even necessary to vary the control parameter continuously in time. Such a change is especially true if a large amount of data has to be accumulated to perform a statistical analysis. The counterintuitive result is that if the control parameter is varied from $\mu<\mu_c$ to $\mu>\mu_c$, the bifurcation point is shifted from μ_c, no matter how slowly μ is varied. This topic has been the subject of numerous investigations devoted to studying the general properties,[7,8] or the specific characteristics of a system,[9] or to exploiting the bifurcation's features for particular applications[10] (for example, the removal of chaotic states and the stabilization of particular orbits). Given the generality of the phenomenon, its far-reaching consequences, and that common intuition suggests the wrong answer, it is worth looking at it in some detail. The fact that a simple and inexpensive experiment can be conducted by students in a junior or senior year lab makes the choice of including it in the undergraduate curriculum compelling.

The purpose of this paper is to present this experiment to introduce the students to delayed (or dynamical) bifurcations by testing some of their basic properties. We suggest that the students first be given the setup and be asked to do the experiment, without previous knowledge of the theory behind it. They will be quite puzzled by the result and be highly receptive when the explanation for the phenomenon is presented in the simple terms we use in this paper. We have chosen to keep the presentation as simple as possible. The instructor can complement our presentation with additional material, including a more rigorous approach to the problem if the students possess adequate background knowledge.

Section II presents the general conceptual framework of the problem, which is developed analytically in a straightforward, but sufficiently complete way in Sec. III. Section IV discusses the experiment using a simple and inexpensive optical setup, and compares the experimental results to the analytical predictions. Some general comments are offered in Sec. V, and specific difficulties encountered by the students are addressed in Sec. VI. A set of questions that can be posed to students is given in Sec. VII, followed by our conclusions in Sec. VIII.

II. CONCEPTUAL FRAMEWORK

One of the most common signatures of nonlinear phenomena is the occurrence of coexisting solutions of nonlinear differential equations. This coexistence may take different forms. One common form of coexistence is hysteresis: three solutions coexist, one of which is always unstable, while the other two may have domains of stability and instability. These solutions are connected by limit points. A second form of coexistence occurs in the vicinity of bifurcation points, where two branches of solutions cross and exchange stability.

In both cases, bistability or, more generally, multistability, is linked to a critical point, either a limit point or a bifurcation point. We shall limit our consideration to stationary solutions, although they can be generalized to time-dependent

states. The multiplicity of solutions requires a stability analysis to determine the stability of the different solutions and their basin of attraction. In general, it is not possible to carry through such an ambitious program. In exceptional cases, some simplified models admit exact solutions and a complete stability analysis is then possible (see Sec. 4.4.1 of Ref. 11 for an example). In most cases, one has to resort to a linear (local) stability analysis, testing the stability of a solution against infinitesimal perturbations. This analysis leads to a characteristic equation for the rates at which the perturbation decays (stable solution) or grows (unstable solution). This characteristic rate may be complex, in which case the decay or the growth of the perturbation is modulated at a frequency given by the imaginary part of the rate. By definition, a critical point is a point where the real part of a rate vanishes, a property common to limit points and bifurcation points.

III. ESCAPING CRITICAL SLOWING DOWN

The inverse of the real part of a characteristic rate is a relaxation time. Hence, a critical point is characterized by an infinite relaxation time. The vicinity of a limit point is characterized by critical slowing down. The magnitude of the relaxation time is controlled by the distance from the critical point; as the critical point is approached, the time scale becomes longer, which means that the dynamics of the system is no longer governed by the usual time scales, such as the atomic relaxation time or the cavity photon lifetime in optics. Rather, the response time is determined by the topological structure and the resulting dynamics is universal. The amount of slowing down can be considerable and in optical systems an increase in time scale by up to six orders of magnitude for the relaxation times has been reported.[12]

Critical slowing down often is unwanted. A classic strategy to evade critical slowing down is to sweep the control parameter across the critical point. The rationale behind this procedure is that if the sweep rate is small enough, the dynamical system should quasi-statically follow the stationary state. This line of reasoning holds far away from critical points, but it turns out to be incorrect close to a critical point.

Let us illustrate these ideas with a simple example that contains all the necessary elements. We consider a system that has two steady states (denoted by a tilde), $\tilde{x}=0$ and $\tilde{x}=A$, where A is the control parameter. We assume that the dynamics of the system can be described by

$$\frac{dx}{dt}=x(A-x). \tag{1}$$

The bifurcation point is at $A=0$. The zero solution is stable if $A<0$ and unstable if $A>0$. Conversely, the solution $\tilde{x}=A$ is unstable if $A<0$ and stable if $A>0$. Figure 1 illustrates the stability exchange (solid line: stable solution; dashed line: unstable one). The bifurcation corresponds to the stability exchange between the two solutions, where the change in behavior of the system passes from a state independent of the value of the control parameter A, because for $A<0$ we always have $\tilde{x}=0$, to one that depends explicitly on A.

We are interested in the transition between the two states when A changes in time, beginning with $A<0$ and crossing the point $A=0$. As long as the solution remains in the neighborhood of $x=0$, a local analysis can be performed by expanding Eq. (1) to first order in the neighborhood of $x=0$

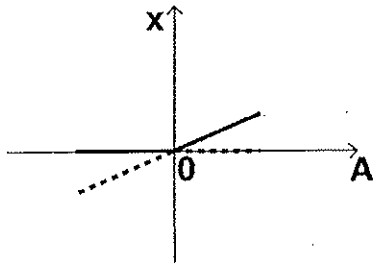

Fig. 1. Steady state solutions of Eq. (1). Stability is denoted by the solid line. The $x=0$ solution is stable for $A<0$, while the $x=A$ solution is stable for $A>0$. The exchange in stability occurs at $A=0$, the (static) bifurcation point.

(that is, $dx/dt=Ax$). To describe the effect of the sweep, we introduce an explicit time-dependence by setting $A=\mu(t)$, so that Eq. (1) becomes $dx/dt=x(\mu(t)-x)$. Notice that $\tilde{x}=0$ remains an exact solution, independent of the functional time dependence of μ. Therefore, the linearized form holds in general, and the evolution is correctly described by

$$\frac{dx}{dt}=\mu(t)x, \tag{2}$$

as long as the solution $x(t)$ remains close to zero. When this solution is no longer valid, the solution $x(t)$ abandons the neighborhood of zero and diverges exponentially, and the transition to a finite value of $x(t)$ has occurred. In this case, Eq. (2) no longer describes the dynamics, but we can characterize the transition by the time at which the solution $x(t)$ starts increasing away from zero. Hence, the operational definition of a dynamical bifurcation, that is, the occurrence of a bifurcation in a time-dependent regime, will be defined as the deviation from the previous, zero solution.

Equation (2) can be formally integrated to obtain the solution

$$x(t)=x(0)\exp\left[\int_0^t \mu(t')dt'\right]. \tag{3}$$

We call $\bar{t}$ the time at which the parameter $\mu(t)$ reaches the bifurcation point. This value is obviously defined by

$$\mu(\bar{t})=0, \tag{4}$$

which determines the static bifurcation, because at this instant the control parameter is zero. The value of the parameter for which

$$x=0, \quad \mu=0, \tag{5}$$

defines the position of the static bifurcation. At time $\bar{t}$ the control parameter reaches the value for which the linear stability analysis predicts a change in stability for the dynamical system. For $t<\bar{t}$, we have $\mu(t)<0$, and therefore $x(t)=0$.

For a time-dependent system, reaching the condition specified by Eq. (4) does not give rise to a change in physical behavior. Indeed, while in the static problem (the result of the usual linear stability analysis where all parameters are kept constant) the point defined by Eq. (5) corresponds to the exchange of stability, in the swept-parameter case the condition $\mu(\bar{t})=0$ does not. We immediately recognize this fact by observing from Eq. (3) that $x(t)$ starts to diverge away from $x(0)$ only when the argument of the exponential func-

tion goes from negative to positive values. For negative values the perturbation relaxes to zero, and only for positive values can it grow from $\bar{x}=0$.

We therefore define another quantity: the *dynamical bifurcation* point, a concept that can exist only if the control parameter is time-dependent. It is defined as the time at which the solution $x(t)$ in Eq. (3) begins to diverge:

$$\int_0^{t^*} \mu(t')dt' = 0. \tag{6}$$

Equation (6) is an implicit equation for the time t^* and can be solved once an explicit form for $\mu(t')$ has been specified. When a solution exists, we can infer some of its basic features from some elementary considerations.

We have assumed that $\mu(t)$ is an increasing function of time, because we want to study the transition from the parameter-independent solution ($\bar{x}=0$) to the other solution. Hence, $\mu(0)<0$. If $\mu(t)$ is monotone (but otherwise generic), we know that until time $\bar{t}$ $\mu(t)\leqslant 0$ for $t<\bar{t}$. Therefore, we are certain that $\int_0^t \mu(t')dt'<0$. As a consequence, at the time the static bifurcation has been reached, the system is still stable on the $\bar{x}=0$ branch. In order for the solution to be destabilized, the integral between $\bar{t}$ and t^* must "accumulate" the right amount of positive "area" to compensate for the "negative" area that has accumulated between 0 and $\bar{t}$:

$$\int_{\bar{t}}^{t^*} \mu(t')dt' = -\int_0^{\bar{t}} \mu(t')dt' = \left| \int_0^{\bar{t}} \mu(t')dt' \right|. \tag{7}$$

Let us illustrate these considerations with an explicit example, where we assume a linear dependence of the control parameter on time:

$$\mu(t) = -A_0 + vt \quad (v, A_0 > 0). \tag{8}$$

Such a dependence is not only convenient mathematically, but also can be implemented experimentally, as discussed in Sec. IV. The integration of Eq. (3) is immediate using Eq. (8), and the conditions given in Eqs. (5) and (6) become:

$$-A_0 + v\bar{t} = 0, \tag{9}$$

$$-A_0 t^* + \frac{v}{2} t^{*2} = 0. \tag{10}$$

From Eqs. (9) and (10) we obtain

$$t^* = 2\bar{t}, \tag{11}$$

$$\mu(t^*) = -\mu(0), \tag{12}$$

and thus the time at which the dynamical bifurcation occurs is twice the time necessary for reaching the static bifurcation, independent of the speed at which the parameter is swept! This result appears to be completely counterintuitive, because one might expect that the sweeping speed v should play a role in the position of the dynamical bifurcation.

A graphical illustration of the results provided by Eqs. (11) and (12) is given in Fig. 2. We see that the area under the triangle in the $\mu<0$ half plane has to be equal to that in the $\mu>0$ half plane [because of Eqs. (6) and (7)]. Because, for ease of illustration (and experimental realization), we have chosen a linear dependence for the parameter, $\mu(t)$, the two triangles of Fig. 2 are equal, and therefore the time necessary

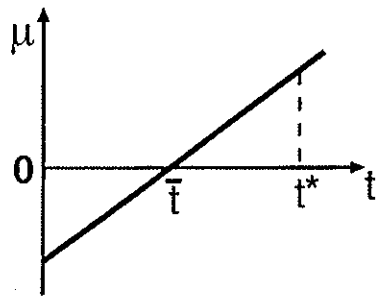

Fig. 2. Illustration of the principle expressed by Eq. (7). The negative area accumulated in the triangle below the t axis (that is, between $t=0$ and $t=\bar{t}$) has to be equal to the positive area accumulated between $t=\bar{t}$ and $t=t^*$ to attain the dynamical bifurcation point.

to reach the dynamical bifurcation is double that of the static one, Eq. (11), independent of the speed v. This condition is a direct consequence of the fact that for the areas to be equal, the value of μ for which the dynamical bifurcation is reached, $\mu(t^*)$, must be equal in absolute value to the initial value of μ, $\mu(0)$.

Another very important point resulting from the analysis is that the time required to reach the static bifurcation $\bar{t}$ (thus also t^*) depends inversely on the sweep rate: $\bar{t}=a_0/v$ (where $A_0>0$ is the initial μ value). Hence, if the sweep is conducted at a slow rate, the time necessary to reach both static and dynamic bifurcation will be correspondingly longer. Although obvious, on the basis of the mathematical derivation, the results provided by Eqs. (8)–(12) are entirely counterintuitive. Indeed, the limit in which the bifurcation is scanned with vanishingly small values of the sweep rate ($v \to 0$) yields a completely different result from the static bifurcation. In the dynamical case the time for reaching the bifurcation diverges ($\bar{t}, t^* \to \infty$), and hence the control parameter value for which it occurs is (mathematically) shifted to infinity. Instead, in the static case the control parameter is kept constant and therefore the position of the bifurcation in parameter space is fixed at its equilibrium value.

What happens in the dynamical case is that there is an accumulation of stability (the integral between 0 and $\bar{t}$), which has to be compensated by going beyond the bifurcation for a certain time. Slowing down the scan only increases the time necessary to achieve the necessary compensation.

Note that the time at which the system loses stability also depends on the initial condition A_0. The larger the magnitude of $|A_0|$, the longer are $\bar{t}$ and t^*, because the system needs more time to reach the static bifurcation and thus has accumulated a greater amount of stability. Therefore, the system can follow the statically unstable solution for a longer time, as illustrated qualitatively in Fig. 3, where the solid line represents the actual trajectory $x(t)$, and as confirmed by the experimental results of Sec. IV [see in particular, Fig. 6(b)]. A comparison of Figs. 3 and 1 shows that the solution has remained on the $x=0$ branch for a longer time than predicted by a static linear stability analysis.

In summary, we see that the limit of the static bifurcation can be approached only by keeping the ratio A_0/v as small as possible. This limit is obtained either by starting the system infinitely close to the threshold (but fluctuations, which are not included in this treatment, will become important, see

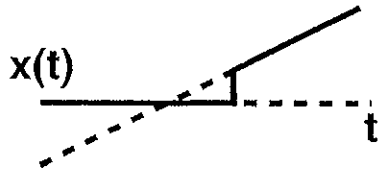

Fig. 3. Dependence of x as a function of the time t when the bifurcation is swept (for increasing values of μ). The static bifurcation point (crossing of the solutions) is passed with $x(t)$ remaining on the unstable solution for some time, before jumping toward the new stable solution. In the opposite sweep x remains on the other solution for a while in spite of its being unstable.

Sec. V), or by using a very large sweep speed, ideally $v \to \infty$. Hence, contrary to intuition, the static bifurcation is approached in the limit in which the system is swept across the bifurcation at infinite speed.

We remark that the long-dashed line in Fig. 3, which illustrates the evolution of $x(t)$ beyond the bounds of validity of our local analysis, is nothing but an educated guess about what $x(t)$ will do after abandoning the $\bar{x}=0$ branch. Indeed, because only one other solution is available, $\bar{x}=A$, and because this solution is stable, it is plausible that the system will converge toward it and that it will do so asymptotically. In Sec. V we will comment on a small difference between this prediction and the experimental situation.

IV. EXPERIMENT

The experimental apparatus is shown in Fig. 4. The output power of a semiconductor laser[13] driven by a modulated/variable power circuit is focused on a solid state detector.[14] The current supplied to the laser is controlled by a standard signal generator. The detector and signal generator outputs are observed with a two-channel digital oscilloscope. The oscilloscope is interfaced to a personal computer to analyze the data. The laser operates in the red region of the optical spectrum ($\lambda \approx 670$ nm, maximum power ≈ 4.2 mW).[15]

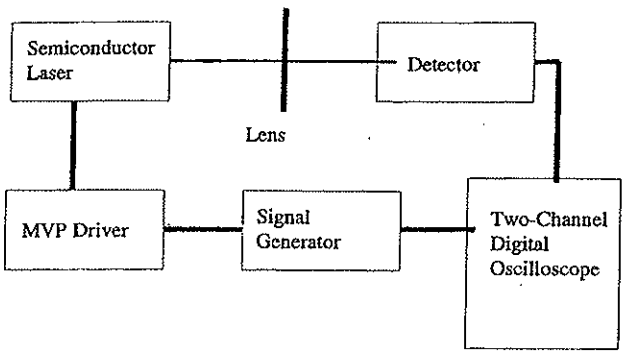

Fig. 4. Schematics of the apparatus. The laser output (see Ref. 13) is focused through a standard lens onto a Si PIN detector (see Ref. 14), connected to a digital oscilloscope (HP54602B digital oscilloscope, 150 MHz, with a HP54657A Measurement/Storage Module HP-IB interface) through a 50 Ω adaptor. The signal from the function generator is simultaneously recorded by the oscilloscope on a second trace. A function generator (Tektronix CFG253, 3 MHz bandwidth) drives the laser through its stabilized power supply (modulated/variable power circuit driver by Thorlabs), which includes protection against junction bias reversal and overvoltage; without input signal, this driver supplies the laser to obtain about 90% of its maximum power.

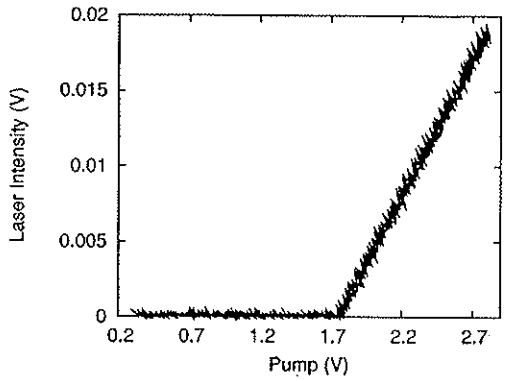

Fig. 5. Laser intensity as a function of pump voltage (signal level from the function generator). The pump voltage changes from 0.3 to 2.8 V. The laser threshold appears for $V=V_{th}=1.78$ V. In this figure and Fig. 6 we plot the data in a way which resembles the oscilloscope's output.

Initially, we determine the threshold voltage and the laser intensity as a function of the pump, that is, the amount of current flowing through the semiconductor junction, injected by the power supply (MVP driver by Thorlabs, cf. Fig. 4), and controlled by the voltage level at the output of the signal generator. We set the offset of the signal generator at around $V_{bias}=+1.55$ V and apply a triangular signal at very low frequency (of the order of 5 Hz) and amplitude 2.5 V (peak-to-peak) to control the injection current. The voltage on the semiconductor laser changes from $V_{min}=+0.3$ V to $V_{max}=+2.8$ V. By setting the oscilloscope in the $x-y$ mode, we can directly observe the laser intensity as a function of pumping voltage.

A typical result is shown in Fig. 5. Several conclusions can be drawn by simple inspection: (i) there exists a pumping value $V_{thr}=+1.78$ V below which the output intensity is constant[16] at $I=0$; (ii) the intensity I grows linearly with the pumping voltage for $V>V_{thr}$; and (iii) the transition from the $I=0$ state to the $I\neq 0$ state appears to be continuous, devoid of hysteresis. In addition, there is no sign of critical slowing down, even though there is an exchange of stability between two different branches. We thus could assume that the measurement is done quasi-statically; the system reaches the steady state value before the parameter changes appreciably. In other words, the experiment appears to show that there is no coexistence of states even close to the bifurcation point (the laser threshold). We will now show that this conclusion is erroneous, and that critical slowing down can be seen by modifying the parameters involved in the measurement.

Without changing the experimental apparatus, we just increase the frequency of the triangular voltage signal to 40 kHz, without modifying its amplitude and bias voltage. In Fig. 6 we show a typical trace of (a) the laser intensity and the pumping voltage as a function of time, and (b) the laser intensity as a function of pumping voltage. We observe that for increasing signal level, the laser switches on at a pumping voltage V^* which is higher than the previously measured V_{thr}. At $V=V^*$, the intensity increases suddenly from 0 to the "large" value, which corresponds to the above-threshold value of the instantaneous pump. This jump is visible in the lower trace of Fig. 6(a), where the laser intensity suddenly grows from the low level (spontaneous emission) to the triangular shape which follows the current injected in the junc-

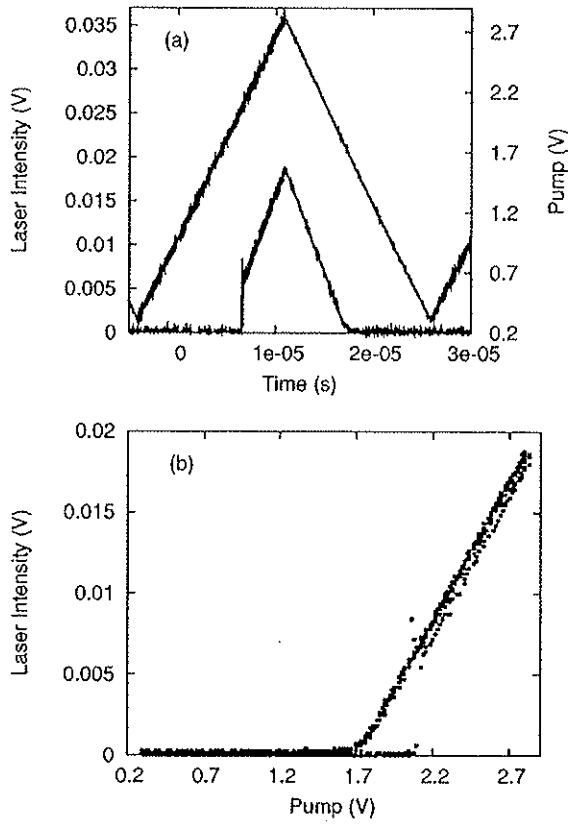

Fig. 6. (a) Laser intensity (bottom trace, left vertical scale) and pump voltage (top trace, right vertical scale) as a function of time for a frequency of the triangle wave applied by the function generator, $f \approx 40$ kHz. In analogy with the notation of Sec. III, V^* represents the voltage value at which the laser switches on (for increasing pump values), while turn-off occurs at $V = V_{th}$ for decreasing pump. In the notation of Sec. III, V_{th} should be expressed as $\bar{V}$. We prefer using the traditional notation V_{th} which is widely recognized in laser physics. (b) Laser intensity as a function of pump voltage. The graph shows bistability in the interval $V_{th} \leqslant V \leqslant V^*$. The traces (plotted with points to better highlight the effect) are slightly separated on the diagonal branch (the lower occurs for increasing pump, the higher for decreasing pump) because of the speed at which the laser is driven.

tion. A comparison of Figs. 6(b) and 3 is very instructive: the delayed jump is visible in the experimental trace (plotted with dots—we suggest that the same be done by using the "dots" options available on most oscilloscopes). As we decrease the voltage, the laser intensity remains proportional to the pumping voltage until it vanishes at $V = V_{thr}$. Thus, there is hysteresis for $V_{thr} < V < V^*$, which can be straightforwardly and clearly displayed using the $x-y$ mode of the oscilloscope [Fig. 6(b)], and shows directly the coexistence of two different states. Notice that there is not a perfect superposition of the traces in the part of the branch where the laser intensity follows the pump [Fig. 6(b)]. This behavior is an artifact of the sweep imposed on the parameter, which prevents the system from being instantaneously at equilibrium: the laser retains a memory of its state at the previous instant, and thus the intensity curve is slightly lower when the pump is being increased and higher when it is being decreased.

Note that the slope of the triangular signal is a direct measurement of the parameter's rate of change and this rate is still orders of magnitude smaller than the smallest relaxation rate of the laser (its relaxation time is in the nanosecond range). Furthermore, the difference $V^* - V_{thr}$ is a direct measurement of the delay time t^* because the voltage is proportional to time. If we keep the amplitude and voltage bias constant, a change in the frequency amounts to only a change in the sweep rate of the pumping parameter.

The theoretical results described in Sec. III show that the time t^* diverges as the sweep rate vanishes. A measurement of the delay time as a function of frequency for the triangular signal should therefore show such behavior. At the same time, if the dynamics are independent of the laser parameters, we should find a universal scaling law for the time t^* as a function of the slope of the triangular function. This prediction can be verified experimentally by measuring the delay time at different scanning frequencies. To do so we keep the amplitude of the modulation constant and simply change the frequency of the triangular wave. Experimentally, we define the delay time as the time starting from the instant at which the triangular wave is at its lowest point, and ending at the instant at which the laser intensity reaches half of its final height (this value is the point with maximum slope, which can therefore be determined most accurately). The measurement of the delay time can be best made by setting the vertical cursors (intensity) at the correct levels (as specified previously) and then using the horizontal ones (time scale) to measure the delay (the oscilloscope's predefined "difference" function will provide the delay time directly).

In Figs. 7(a) and 7(b) we plot t^* as a function of $b = dV/dt$, and $\ln(t^*)$ as a function of $\ln(b)$,[17] for different amplitudes and bias voltages. From the plots we conclude that the delay time increases as we decrease the sweep rate and that it diverges for a vanishing sweep rate. Thus, critical slowing down exists at the bifurcation point. Furthermore, the scaling law is of the type $t^* = Cb^x$, where x is independent of the laser parameters and the constant C depends on the amplitude and bias voltage of the triangular signal. We also remark that the scaling law breaks down for large values of the sweep rate and/or V_{min} relatively close to threshold.

V. COMMENTS

This brief section is devoted to a more detailed discussion of some finer points related to the comparison between the paradigmatic model for a dynamical bifurcation, discussed in Sec. III, and the measurements performed on our system. These points are not apparent in our figures, but will become obvious to anyone repeating the experiment and looking for these effects.

As mentioned in Sec. III, if V_{min} is set close to threshold, the system becomes sensitive to noise. In this case, the scaling exponent that we have derived with the simple model cannot hold (see Sec. VI), because noise has not been taken into account. For this reason we cannot reach the limit $A_0/v \to 0$ by choosing a very small value for A_0. There is another reason that restricts the approximation of $dx/dt = x(\mu - x)$ by $dx/dt = \mu x$ to the domain $x \ll 0$. If x is a small quantity, say ε, then the linearized equation $dx/dt = \mu x$ is balanced only if μ is not small. That is, each member of the equation is proportional to ε. However, if A_0 also is a small quantity, comparable to ε, then the right-hand side μx is proportional to ε^2 for small times while the left-hand side remains proportional to ε. This dependence is inconsistent,

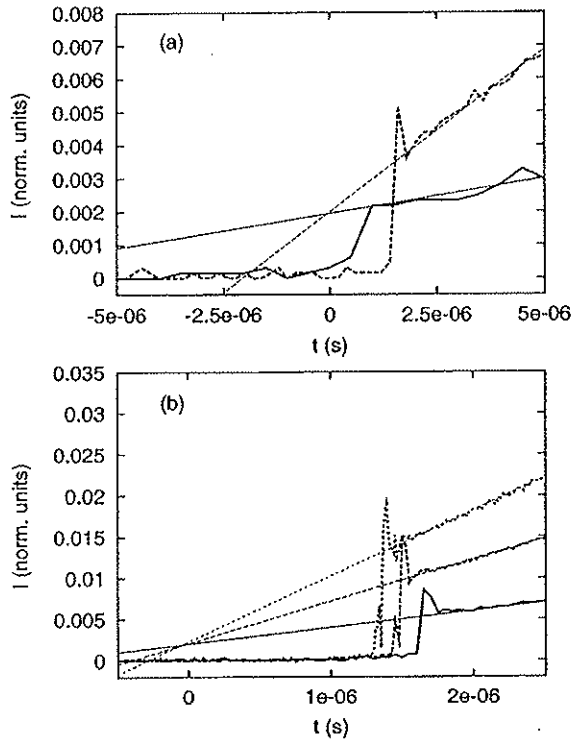

Fig. 9. (a) and (b) The variation of the delay at the bifurcation starting from the instant when the driving signal (triangle wave) crosses threshold. This choice provides the best visualization but is not the best choice for measuring the delay—see the text. In (a) the solid line represents the laser response at $f=3$ kHz, the dashed line at $f=10$ kHz. The curve at $f=1$ kHz has too low a resolution (see the text) and is not shown. The straight lines are superimposed on the linear part of the laser intensity response and are intended to guide the eye to show the expected behavior of the laser intensity in the absence of a delayed bifurcation. The shift toward positive values of the intensity of the crossing point of the straight lines (at the trigger time) is discussed in the text. (b) Same as (a) for $f=20$ kHz (solid line), $f=50$ kHz (long-dashed line), and $f=80$ kHz (short-dashed line). A reduction in the delay time for increasing frequency f is clearly visible throughout the graphs [notice the change in horizontal scale between (a) and (b)].

VII. QUESTIONS FOR STUDENTS

We offer a few questions that can be posed to students to test their degree of understanding of the physics behind the experiment and their mastery of the techniques involved.

(1) If the delay in reaching the bifurcation point grows when reducing the frequency, then why was the static threshold determined by using a very slow ramp (≈ 5 Hz in Sec. IV)?
(2) Is it possible in practice to obtain an actual measurement of the true static threshold in a real experiment? Justify your answer.
(3) Why aren't the experimental delay times measured from the point where the laser threshold is crossed?
(4) Compare the measurement of the delay time taken from the initial instant of the ramp to (a) a set threshold intensity value (any value between minimum and maximum intensity on the switch-on); (b) the mid-point of the rising intensity front (see Sec. IV); and (c) the zero-crossing of the laser intensity derivative (see Ref. 23). What are the advantages and the disadvantages of each technique?
(5) Would it be a good idea to set the trigger level in such a way as to start the trace at the point from which we want to measure the delay (the bottom point of the triangle wave)? This procedure would avoid having to use the pretrigger and the cursors (at least one of them), because we could read the time directly off the oscilloscope's scale. Comment on this procedure and explain which is the best choice.
(6) Why are Figs. 8 and 9 taken with the trigger set close to threshold for better visualization purposes?

VIII. CONCLUSION

We have shown that sweeping a control parameter across a critical point does not bypass critical slowing down. We did so by solving a simple analytic model and by conducting an experiment involving a semiconductor laser and standard lab equipment.

Although we have concentrated on the simplest aspect of the delay problem, generalizations are quite obvious. Experimentally, we could ask if t^* vanishes for large values of the sweep rate. Intuitively we would say that if b is sufficiently large, the delay time becomes equal to the response time of the system, and therefore independent of the sweep rate. This effect, that is the dependence of the response time of the system on the initial pumping value—the "memory time"—and the dependence of the first peak amplitude on the delay time, can be easily measured in a similar experiment, but will be the subject of future work. We note that the linear equation (2) can still be solved analytically if we add a constant term (modeling an imperfection), a modulation, or noise. These generalizations are discussed in Ref. 11. Finally, whether we deal with a first- or second-order phase transition-like model does not change any of our conclusions.

Another generalization is provided by optically bistable systems.[29] In this case, the minimal equation, Eq. (1), must have a cubic nonlinearity and therefore the dependence on the sweep rate will be characterized by different exponents. The basic problem remains the same: sweeping across a critical point (here, a limit point) induces a delay generated by critical slowing down and the dynamical hysteresis is larger than the static one.

ACKNOWLEDGMENTS

The work in Brussels was supported by the Fonds National de la Recherche Scientifique and the Interuniversity Attraction Pole program of the Belgian government. We are grateful to M. Giudici for comments and discussions.

[a]Corresponding author; electronic mail: Gian-Luca.Lippi@inln.cnrs.fr
[b]Undergraduate student at the Department of Physics at the time of the work.

[1]N. B. Tufillaro and A. M. Albano, "Chaotic dynamics of a bouncing ball," Am. J. Phys. **54**, 939–944 (1986); T. M. Mello and N. B. Tufillaro, "Strange attractors of a bouncing ball," *ibid.* **55**, 316–320 (1987); H. T. Savage, C. Adler, S. S. Antman, and M. Melamud, "Static and dynamic bifurcations in magnetoelastic ribbons," J. Appl. Phys. **61**, 3802 (1987); O. Maldonado, M. Markus, and B. Hess, "Coexistence of three attractors and hysteresis jumps in a chaotic spinning top," Phys. Lett. A **144**, 153–158 (1990); S. T. Vohra, F. Bucholtz, D. M. Dagenais, and K. P. Koo, "Direct observation of dynamic strain bifurcations and chaos in magnetostrictive amorphous ribbons," J. Appl. Phys. **69**, 5736–5738 (1991).
[2]S. M. Rezende, A. Azevedo, A. Cascon, and J. Koiller, "Organizing centers of bifurcations in spin-wave instabilities," J. Appl. Phys. **69**, 5430–5435 (1991); D. J. Mar, L. M. Pecora, F. J. Rachford, and T. L. Carrol,

"Dynamics of transients in yttrium-iron-garnet," Chaos 7, 803–809 (1997).
[3]G. Nicolis and I. Prigogine, *Self-Organization in Non-Equilibrium Systems* (Wiley, New York, 1977); J.-C. Roux, "Experimental studies of bifurcations leading to chaos in the Belousov-Zhabotinsky reactions," Physica D 7, 57–68 (1983); J. L. Hudson and O. E. Rössler, "Chaos and complex oscillations in stirred chemical reactions," in *Dynamics of Nonlinear Systems*, edited by V. Hlavacek (Gordon & Breach, New York, 1985).
[4]C. Normand, Y. Pomeau, and M. G. Velarde, "Convective instability: A physicist's approach," Rev. Mod. Phys. **49**, 581–624 (1977); P. Bergé, Y. Pomeau, and Ch. Vidal, *Order within Chaos* (Wiley, New York, 1984); R. P. Behringer, "Rayleigh-Bénard convection and turbulence in liquid helium," Rev. Mod. Phys. **57**, 657–687 (1985).
[5]The literature is too extended to be cited here. A good overview of the problem is presented in H. Haken, "Cooperative phenomena in systems far from thermal equilibrium and in nonphysical systems," Rev. Mod. Phys. **47**, 67–121 (1975), which also contains other interesting examples.
[6]H. G. Solari, M. A. Natiello, and G. B. Mindlin, *Nonlinear Dynamics* (IOP, Bristol, UK, 1996); S. H. Strogatz, *Nonlinear Dynamics and Chaos: With Applications to Physics, Biology, Chemistry and Engineering* (Perseus, Cambridge, MA, 2001).
[7]F. De Pasquale, Z. Racz, M. San Miguel, and P. Tartaglia, "Fluctuations and limit of metastability in a periodically driven unstable system," Phys. Rev. B **30**, 5228–5238 (1984); R. Kapral and P. Mandel, "Bifurcation structure of the nonautonomous quadratic map," Phys. Rev. A **32**, 1076–1081 (1985); G. Broggi, A. Colombo, L. A. Lugiato, and P. Mandel, "Influence of white noise on delayed bifurcations," *ibid.* **33**, 3635–3637 (1986); C. Van den Broeck and P. Mandel, "Delayed bifurcations in the presence of noise," Phys. Lett. A **122**, 36–38 (1987).
[8]H. Zeghlache, P. Mandel, and C. Van den Broeck, "Influence of noise on delayed bifurcations," Phys. Rev. A **40**, 286–294 (1989).
[9]P. Mandel and T. Erneux, "Laser Lorenz equations with a time-dependent parameter," Phys. Rev. Lett. **53**, 1818–1820 (1984); M. Lefebvre, D. Dangoisse, and P. Glorieux, "Transients in far-infrared laser," Phys. Rev. A **29**, 758–767 (1984); L. Fronzoni, F. Moss, and P. V. E. McClintock, "Swept-parameter-induced postponements and noise on the Hopf bifurcation," *ibid.* **36**, 1492–1494 (1987); W. Scharpf, M. Squicciarini, D. Bromley, C. Green, J. R. Tredicce, and L. M. Narducci, "Experimental observation of a delayed bifurcation at the threshold of an argon laser," Opt. Commun. **63**, 344–348 (1987); M. C. Torrent and M. San Miguel, "Stochastic-dynamics characterization of delayed laser threshold instability with swept control parameter," Phys. Rev. A **38**, 245–251 (1988); F. T. Arecchi, W. Gadomski, R. Meucci, and J. A. Roversi, "Dynamics of laser buildup from quantum noise," *ibid.* **39**, 4004–4015 (1989); S. T. Vohra, F. Bucholtz, K. P. Koo, and D. M. Dagenais, "Experimental observation of period-doubling suppression in the strain dynamics of a magnetostrictive ribbon," Phys. Rev. Lett. **66**, 212–215 (1991); D. Bromley, E. J. D'Angelo, H. Grassi, C. Mathis, and J. R. Tredicce, "Anticipation of the switch-off and delay of the switch-on of a laser with a swept parameter," Opt. Commun. **99**, 65–70 (1993); S. T. Vohra, L. Fabiny, and K. Wiesenfeld, "Observation of induced subcritical bifurcation by near-resonant perturbation," Phys. Rev. Lett. **72**, 1333–1336 (1994).
[10]V. N. Chizhevsky and P. Glorieux, "Targeting unstable periodic orbits," Phys. Rev. E **51**, R2701–R2704 (1995); V. N. Chizhevsky, R. Corbalán, and A. N. Pisarchik, "Attractor splitting induced by resonant perturbations," *ibid.* **56**, 1580–1584 (1997); K. Pyragas, "Control of chaos via an unstable delayed feedback controller," Phys. Rev. Lett. **86**, 2265–2268 (2001).
[11]P. Mandel, *Theoretical Problems in Cavity Nonlinear Optics* (Cambridge U.P., New York, 1997).
[12]J. Y. Bigot, A. Daunois, and P. Mandel, "Slowing down far from the limit points in optical bistability," Phys. Lett. A **123**, 123–127 (1987).
[13]The laser is a modulated visible laser diode kit, Thorlabs, Model S1031, ≈$250. A stabilized power supply can be purchased for this system from the same manufacturer. The modulating signal is coupled, from a standard function generator, directly into the laser circuit with a jack connector.
[14]High Speed Silicon Detector, 1 GHz bandwidth, Model DET 210 by Thorlabs, ≈$100.
[15]This system is no longer sold by Thorlabs and we do not know of another company selling this device. A possible replacement for this laser system could be the PMA Laser Module by Power Technology, ⟨www.powertechnology.com⟩: a laser module with built-in analogic modulation and the protections which are necessary to make it a useful student lab tool.
[16]The spontaneous emission, always present in measurable amounts in semiconductor lasers, is not considered here. In practice, no special operation is required, because the spontaneous contribution remains hidden in the trace noise of the oscilloscope when the vertical amplification is correctly chosen for the visualization of the lasing output.
[17]The logarithmic functions are natural logarithms throughout the paper.
[18]A discussion for class B lasers (Ref. 19) can be found in Sec. V.A of Ref. 20 (read the commentary to Figs. 6 and 7 in that section).
[19]J. R. Tredicce, F. T. Arecchi, G. L. Lippi, and G. P. Puccioni, "Instabilities in lasers with an injected signal," J. Opt. Soc. Am. B **2**, 173–183 (1985).
[20]G. L. Lippi, L. M. Hoffer, and G. P. Puccioni, "Noise at the turn-on of a class-B laser," Phys. Rev. A **56**, 2361–2372 (1997).
[21]The horizontal scale used in Fig. 6(b), chosen to display a whole period of the triangular driving, does not possess enough resolution to show the detail of the transition: an overshoot of the intensity beyond the triangular shape, with damped oscillations. This can only be seen by triggering around V^* and expanding the scale. However, one can recognize an indication of a more complex evolution from the jagged trace at the sharp front.
[22]We remark that some students, even very bright ones, will oscillate between considering the explanation obvious, when looking at the theory, and totally wrong, when sitting in front of the experiment. It may take some time and patient discussion to convince them of the fact that the experimental results truly agree with the theoretical interpretation and that their intuition and some of the experimental visualizations suggest the wrong conclusion.
[23]With digital oscilloscopes that provide the derivative of the signal, it is possible to use this feature (when the detector signal is not too noisy), to determine the "end-time" for the measurement of the delay. The derivative changes sign at the inflection point of the switch-up, a point that depends directly on the signal shape rather than on a threshold level set by the user. The advantage of this measurement technique, relative to the mid-height reference that we have discussed so far, is that the oscilloscope provides the end-time information without further manipulation by the user; its disadvantage is that if the signal is too noisy, then the information coming from the derivative may be difficult to exploit. In the tests we performed, however, the zero crossing of the intensity derivative always proved to be a reliable indicator.
[24]D. Bromley, E. J. D'Angelo, H. Grassi, C. Mathis, J. R. Tredicce, and S. Balle, "Anticipation of the switch-off and delay of the switch-on of a laser with a swept parameter," Opt. Commun. **99**, 65–70 (1993).
[25]This upward shift in the crossing point to nonzero intensity values is related to the fact that due to the continuous sweep, the laser maintains a certain degree of memory of its state at the previous instant. As a consequence, the initial slope of the laser intensity versus time is smaller than it ought to be, and the extrapolated straight lines meet at a nonzero vertical coordinate. A discussion of the various consequences on the output intensity of a class-B laser of sweeping the pump can be found in Ref. 24. As an illustration, the flatter slope in the initial phases of lasing for growing pump values can be recognized clearly in Fig. 6(b), where the linear response regime appears to be doubled; the upsweep corresponds to the lower of the two curves. In Fig. 8 the same effect is less visible because of the scale on which the curves are plotted.
[26]G. P. Agrawal and N. K. Dutta, *Long-Wavelength Semiconductor Lasers* (Van Nostrand-Reinhold, New York, 1986).
[27]W. Scharpf, M. Squicciarini, D. Bromley, C. Green, J. R. Tredicce, and L. M. Narducci, in Ref. 9.
[28]In a semiconductor laser, as in all Class B lasers (Ref. 19), the excess population inversion necessary to initiate the optical amplification process gives rise to an additional macroscopic time delay. A discussion of this contribution, which is nonlinear and is expected to deform the distribution of points measured in Fig. 7, is beyond the scope of this paper. An understanding of its physical origin can be gained from Sec. V.A of Ref. 20.
[29]P. Jung, G. Gray, R. Roy, and P. Mandel, "Scaling law for dynamical hysteresis," Phys. Rev. Lett. **65**, 1873–1876 (1990); J. Zemmouri, B. Ségard, W. Sergent, and B. Macke, "Hesitation phenomenon in dynamical hysteresis," *ibid.* **70**, 1135–1138 (1993).

ComPlexUs

ORIGINAL RESEARCH PAPER

ComPlexUs 2003;2:101–111; DOI: 22988476097

Received: October 19, 2001

Accepted after revision: September 19, 2002

Bursting Oscillations in Two Coupled FitzHugh-Nagumo Systems

Catherine Doss-Bachelet Jean-Pierre Françoise Claude Piquet

Géométrie Différentielle, Systèmes Différentiels, Imagerie Géométrique et Biomédicale, Université de Paris VI, Paris, France

Key Words

Bifurcation theory · Fast - slow dynamics · Bursting oscillations · Excitability

Abstract

The purpose of this short article is to show that bursting oscillations occur naturally in two coupled FitzHugh-Nagumo systems. As far as we know, this has not been observed previously. We gradually came to this conclusion after a discussion (reproduced herein) of known examples where these oscillations have been described in biological systems. Bursting activity typically is the result of the interaction of a fast excitatory subsystem and a slow subsystem. We consider here three different time scales. The fast excitatory subsystem is itself a 'fast-slow' dynamics. The special pattern of the bursting oscillations obtained (appearance of a transitory bump between the spiking phase and the silent phases) is discussed in the framework of qualitative plane analysis and geometric singular perturbation theory.

Fax +41 61 306 12 34
E-Mail karger@karger.ch
www.karger.com

KARGER

©2003 S. Karger AG, Basel
1424–8492/03/0013–0101
$19.50/0
Accessible online at:
www.karger.com/cpu

Pr. Jean-Pierre Françoise
Université P.-M. Curie, Paris VI,
Imagerie Géométrique et Biomédicale, Site Chevaleret
175, Rue du Chevaleret, F–75013 Paris, France
Tel. +33 144 278561, Fax +33 144 275332, E-Mail: jpf@ccr.jussieu.fr

Synopsis

In general use, the word 'bifurcation' invokes the notion of branching. In its mathematical sense, the word has a more specific meaning. As V.I. Arnold described it in 1972, the word bifurcation *"is widely used to describe any situation in which the qualitative, topological picture of the object we are studying alters with a change of the parameters on which the object depends. The objects in question can be extremely diverse: for example, real or complex curves or surfaces, functions or maps, manifolds or fibrations, vector fields, differential or integral equations"* [25].

Most recently, bifurcation theory has paid dividends in the analysis of differential equations; indeed, over the past three decades or so, mathematical techniques gathered under this name have offered a powerful means for exploring nonlinear phenomena in diverse settings, ranging from interacting biological populations and cardiac dynamics to fluid turbulence, oceanic flows and pattern formation in systems driven away from equilibrium. Bifurcation theory forgoes the attempt to find exact analytical solutions to a system of dynamical equations; rather, it seeks to elucidate generic qualitative features of the solutions, and so provide insight into the origins of important dynamical phenomena. A central motif of both bifurcation theory and modern dynamical systems theory is that apparently diverse systems often have similar dynamics. Moreover, these dynamics can often be understood in terms of greatly simplified dynamical models of low dimension; that is, models having only a few variables.

In their article, Doss-Bachelet et al. explore this approach in connection with so-called bursting dynamics – a widespread phenomenon in biological systems. In pancreatic β-cells, for example, the membrane potential often fluctuates in a highly complex but distinctive manner – with bursts of high-frequency oscillations episodically punctuating far quieter peri-

Introduction and Outline of Results

One of the first models for bursting for the oscillatory behavior in electrical activity from pancreatic β-cells was proposed by Atwater et al. [1]. This was later developed into a mathematical model by Chay and Keizer [2]. The simplified model of Rinzel and Lee [3] can be analyzed with the qualitative bifurcation theory. The fast dynamics depends on a parameter c. For certain values of the parameter, the system displays three equilibria. One attractor of node type, a limit cycle which contains an unstable focus in the interior, and a saddle point. The slow dynamics drives the parameter c in such a way that an initial point is first attracted to the node (quiescent phase). Then the node disappears into a saddle-node bifurcation and thus the initial point is attracted by the limit cycle and it undergoes very quickly (fast dynamics) an oscillation (active phase) for some time (several spikes) until the limit cycle disappears into a homoclinic bifurcation. The flow then goes back to the attractive node and recovers the quiescent phase, and so on repeatedly. There are thus two ingredients to explain the important features of the bursting oscillations: the singular peturbation aspect with the fast-flow dynamics, and the qualitative plane dynamics which displays two bifurcations, namely the homoclinic bifurcation and the saddle-node bifurcation.

Although bursting has been studied extensively for many years, most mathematical studies are based on the pioneering work of Rinzel [4]. Rinzel's interpretation of bursting in terms of nonlinear dynamics is one of the most successful stories of mathematical physiology. Rinzel proposed a classification of burstings (of interest in medecine) that we reproduce here to make this article self-contained.

Type 1. The active phase begins at a saddle-node bifurcation and ends at a homoclinic bifurcation. In types 1a (fig. 1a) and 1b, the minimum of the burst lies above and below the quiescent phase, respectively. The spike period increases monotonically through the active phase. The slow dynamics is one-dimensional and yields a hysteresis.

Type 2. The active phase begins and ends at a homoclinic bifurcation. The bursting oscillations look symmetrical and as such are named parabolic. The slow dynamics is two-dimensional and oscillatory.

Type 3. The active phase begins at a Hopf bifurcation and ends at a saddle-node of periodics (collapsing of a stable and of an unstable limit cycle, fig. 1b). Slow dynamics displays a hysteresis. Damped oscillations appear at one extremity and as such this type of bursting is sometimes called elliptic.

Recent contributions to bursting were concerned with the analysis of the mechanism which in the fast system gives birth to repetitive spiking. A new classification based on different types of bifurcations was considered in Wang and Rinzel [5], Bertram et al. [6] and Hoppensteadt and Izhikevich [7]. Pernarowski's model [8] which is analogous to biophysical models of bursting activity in pancreatic β-cells, ods in which the potential remains unchanged. Similar bursting dynamics have been observed also in neurons and in cardiac cells. What is the origin of this general dynamical behavior? As Doss-Bachelet et al. show, a class of dynamical models based on the FitzHugh-Nagumo system of equations naturally exhibit bursting behavior of this kind. While many other dynamical models also produce bursting dynamics, the models explored here are simpler. Moreover, as the FitzHugh-Nagumo equations can be derived from the Hodgkin-Huxley equations – a classic system known to describe the propagation of impulses along nerve axons – they may be more closely tied to systems of biological relevance.

Understanding the authors' approach requires a rudimentary understanding of the elements of bifurcation theory as applied to differential equations [26]. Hence, a few paragraphs of review are in order. As an illustrative example, consider the equation $dx/dt = \lambda - x^2$, where λ is a parameter. Bifurcation theory aims to explore how points flow about in *phase space*, i.e. the domain of the variable x. (In this one-dimensional example, the phase space is the set of points $-\infty < x < \infty$; for a system of coupled equations involving two variables x and y, the phase space would be the entire $x-y$ plane, and so on.) Understanding the topology of the flow or movement of points in this phase space is equivalent to forming a qualitative understanding of the system's solution.

Curiously, the flow is most easily identified by first finding those points that do not flow, the so-called *fixed points* (or equilibrium points). In this one-dimensional example, these are points x_f for which $dx/dt = 0$. To begin with, suppose that $\lambda > 0$. By setting $dx/dt = \lambda - x^2 = 0$, we find two fixed points, $x_f = \pm\sqrt{\lambda}$. Taking the analysis further, one can show that the fixed point at $+\sqrt{\lambda}$ is stable in the sense that all nearby points flow toward it, while the fixed point at $-\sqrt{\lambda}$ is unstable, i.e. all

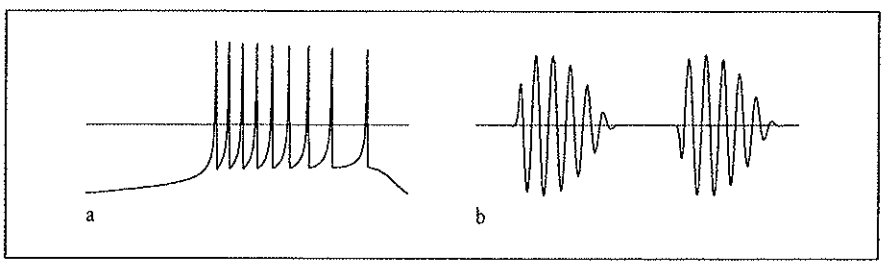

Fig. 1. Example of type 1 (a) and type 3 bursting (b).

is obtained from the interaction of the Danglemayr-Guckenheimer [9] system (fast) and a slow system. It shares with our example the property of being polynomial and hence suitable for the application of qualitative analysis [10].

For the convenience of the reader, the reference list contains useful discussions of singular Hopf bifurcation with fast-slow variables [11, 12].

Similar results are obtained when the slow variables oscillate independently of the fast variables, acting as a periodic driver of the fast system [13, 14].

We consider this type of slow dynamics in this article. The slow dynamics is either periodic (harmonic osciallator, piece-wise linear dynamics) or displays an oscillatory behavior of limit cycle type (van der Pol or FitzHugh-Nagumo). The fast dynamics (which is itself a fast-slow dynamics) is of bistability type, although there is a single equilibrium position and the bistability relates to the excitability nature of the attractor. This model is also close to the models studied in Holden and Erneux [15] where a slow passage through a Hopf bifurcation models an enzymatic reaction. Our model looks simpler and paradigmatic of bursting oscillations, although some types of bursting osciallations may not be produced by forcing excitable systems. The main novelty of this article is that the slow dynamics may be of limit cycle type (relaxation oscillations), and in particular we emphasize the fact that bursting oscillations appear quite naturally in this framework for two coupled FitzHugh-Nagumo equations. Some comments on the methodology could be useful to readers not acquainted with the field of modelling oscillatory behavior with this paradigm. Several methods of investigation have been developed in the study of forcing plane oscillators. Qualitative analysis of projections of orbits on the plane phase ranks among the most commonly used to supplement the graphical representation of the waveform. Numerical simulation adds new insights and allows exploration of a full range of parameters. Dynamical systems theory provides appropriated keys to the interpretation of the simulation data.

The FitzHugh-Nagumo System and Its Excitability

The Hodgkin-Huxley approach [16] explained the formation and the propagation of the nerve impulse along the giant squid axon and initiated many other models in modern electrophysiology, e.g. cardiac rythm and neurodynamics. This approach yields a nonlinear partial differential equation coupled with a dynamical system. A natural limit of this system displays the FitzHugh-Nagumo equation. We recall here a classic analysis of the FitzHugh-Nagumo system, e.g. Keener and Sneyd [17]. We specify the parameters as follows:

$$\begin{aligned} \varepsilon \dot{x} &= -y + 4x - x^3, \\ \delta \dot{y} &= x - by - c. \end{aligned} \tag{2.1}$$

First choose $b = 0$ and $c = c_0 = -2/\sqrt{3}$. The cubic nullcline $y = f(x) = 4x - x^3$ has a local minimum for $x = c_0$ and a local maximum for $x = -c_0$. The differential system (e.g. 2.1) has a unique equilibrium point $(x_0, y_0) = (c_0, f(c_0))$. Then we move slightly the position of the linear nullcline and consider:

$$\begin{aligned} \varepsilon \dot{x} &= -y + f(x), \\ \delta \dot{y} &= x - \Delta - c_0, \end{aligned} \tag{2.2}$$

with Δ small ($\Delta < 2(\varepsilon/\delta)^{1/2}$). The system (e.g. 2.2) still has a unique equilibrium position (x_1, y_1). Linearization of the vector field (e.g. 2.2) around that point shows that this equilibrium position is an attractive focus if $\Delta < 0$ and a repulsive focus if $\Delta > 0$. There is thus a change of stability at the bifurcation $\Delta = 0$. If the ratio ε/δ is small, the fast-slow dynamics displays the patterns shown in figure 2a, b.

In case of $\Delta < 0$, there is only one attractive focus, and for some points near the equilibrium position and above the nearby points flow away from it. This flow is easily depicted with some arrows within the phase space.

But this is only for $\lambda > 0$. Clearly, if $\lambda < 0$, then the system has no fixed points. In this case, we find $dx/dt < 0$ everywhere, and flow is unidirectional – always toward smaller values of x.

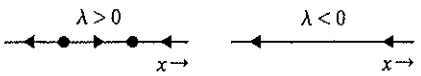

Hence, the topology of the flow changes suddenly at $\lambda = 0$ – an example of a bifurcation. The consequences of this bifurcation can be depicted visually by plotting the positions of the fixed points versus the parameter λ, marking the location of the stable fixed point with a solid line and the unstable with a dashed line.

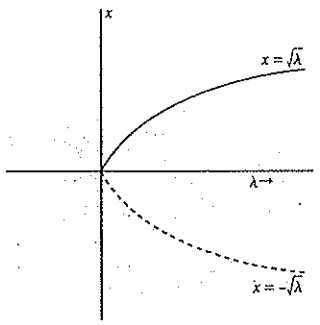

As λ decreases through zero the two fixed points collide and annihilate one another in a generic pattern known as a *saddle-node bifurcation.*

In systems of more than one dimension, fixed points also characterize the flows, although here the possibilities are more diverse. In two dimensions, a fixed point is *stable* (or *attracting*) if all points in the vicinity flow asymptotically toward it, and *unstable* (or *repelling*) if they flow away. An unstable fixed point may be unstable in all directions, or, alternatively, it may be that nearby points flow in along one direction, but out along another. This latter case is known as a *saddle point.*

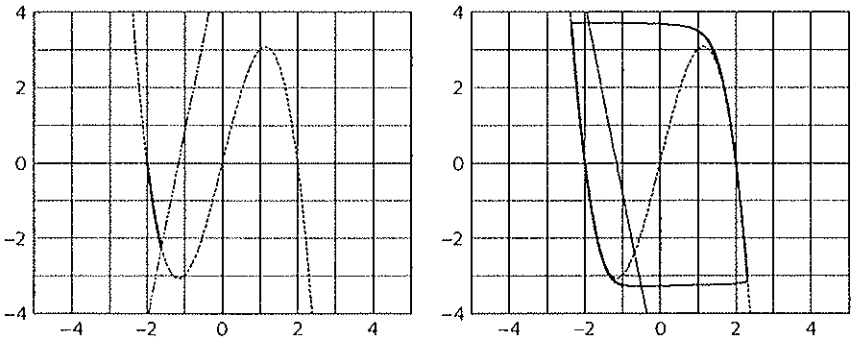

Fig. 2. Examples of FitzHugh-Nagumo fast-slow dynamic patterns. a Attractive singular point. b Attractive limit cycle.

cubic nullcline, the flow is quickly attracted to the focus. Instead for some other points (x, y) still near the equilibrium position but below the threshold $(x, f(c_0))$, the flow undergoes a rather long path before going back to the attractive focus. This special feature has little to do with qualitative dynamics but is strongly related to the singular perturbation analysis and the so-called excitability of the stable equilibrium position.

In case of $\Delta > 0$, the equilibrium position becomes unstable. Under the influence of the fast-slow dynamics, the point jumps until it intersects the cubic nullcline. Then it goes up slowly along the cubic nullcline until it reaches the local maxima. There, under the influence of the fast dynamics, it is pushed back to the other branch of the cubic. It then returns slowly to almost the equilibrium position and then starts again. This shows that an attractive limit cycle has been born in the bifurcation. The bifurcation is thus a supercritical Hopf bifurcation [18]. The classic phase plane analysis has to be adapted to the singular perturbation context [12].

We propose to generate the bursting oscillations by coupling the dynamics (e.g. 2.2, with b small) with a dynamics on the parameters b (or c), which makes the linear nullcline oscillate back and forth relative to the line $x = c_0$.

Two situations are considered. In the first, the slow dynamics that drives b or c is the harmonic oscillator or produced by a piece-wise linear dynamics. In the second, the periodic oscillation of b is a limit cycle (relaxation oscillation) with the van der Pol equation or the FitzHugh-Nagumo system. Sometimes, the bursting oscillations are followed by damped oscillations or by a plateau. We discuss the appearance of such an intermediate state in terms of qualitative dynamics.

The Slow Dynamics Is Oscillatory

Consider the first system:

$$\begin{aligned} \varepsilon\dot{x} &= -y + 4x - x^3, \\ \delta\dot{y} &= x - b(t)y - c_0, \\ b(t) &= a\sin(\omega t), \end{aligned} \qquad (3.1)$$

with the following values of the parameters:

$$\varepsilon = 0.25 \times 10^{-3}, \delta = 0.6 \times 10^{-3}, c_0 = -2/\sqrt{3}$$

and we vary the period $T = 2\pi/\omega$. Note that the ratio ε/δ is not small, hence the initial system is close to a van der Pol oscillator. Since ε and δ are both quite small, the forcing system can be considered as slow. We apply the methodology described in the introduction and draw the wave form and the corresponding projection of the orbits in the phase plane. From the wave form, the possibility to generate

Bifurcation theory categorizes the kinds of bifurcations that typically occur in dynamical systems; in two dimensions, the simplest possibility follows the same *saddle-node* pattern as in the 1D example just considered (indeed, the name of this bifurcation comes from the 2D setting). In a system with both a stable node and a saddle, these may come together with the variation of a parameter and annihilate one another; or, varying the parameter in the opposing sense, they would be born together.

There are many richer possibilities as well – and one of these plays a central role in Doss-Bachelet et al.'s model of bursting dynamics. When a stable fixed point loses its stability, the process may involve the birth of a new periodic orbit – a trajectory forming a closed loop – in a process known as a *Hopf bifurcation*. If on one side of the bifurcation the fixed point is stable, with all nearby points flowing toward it, then on the other the fixed point will be unstable, with nearby points flowing away from it and eventually approaching the new periodic trajectory – also known as a *limit cycle*.

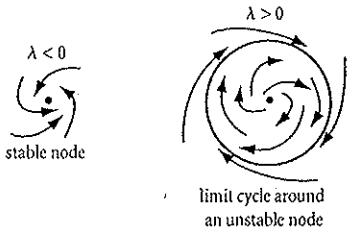

A third generic possibility in 2D is a so-called *homoclinic bifurcation*, which again leads to the birth (or disappearance) of a periodic orbit. Although the mathematical analysis of this bifurcation is more involved, the qualitative transformation is fairly simple. Suppose a system has both a saddle point and a stable fixed point. Typically, the trajectories that enter and leave the saddle will represent distinct trajectories that fail to connect to one another. On variation of a parameter, however, they may at some point meet and form a

bursting oscillations appears clearly. Variation of the parameters allows to change the number of spikes. This system exhibits the solutions (for different values of T and $a = 0.2$) shown in figure 3.

We discuss the dependency in terms of the ratio ε/δ and the amplitude a. We first fix $a = 0.2$, $T = 0.2$, $\varepsilon = 0.25 \times 10^{-3}$ and vary δ (fig. 4), which shows that the number of spikes decreases when ε/δ decreases.

Now choosing $\varepsilon = 0.25 \times 10^{-3}$ and $\delta = 0.6 \times 10^{-3}$. The period T being equal to 0.10, we increase a from 0.05 to 0.20 (for a greater than 0.30, there is no bursting at all) and get the oscillations shown in figure 5.

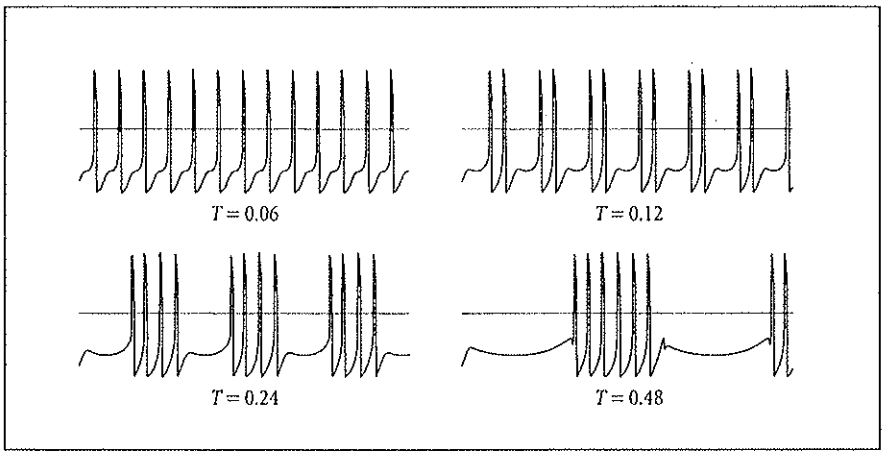

Fig. 3. Dependency of the number of spikes in terms of the period T.

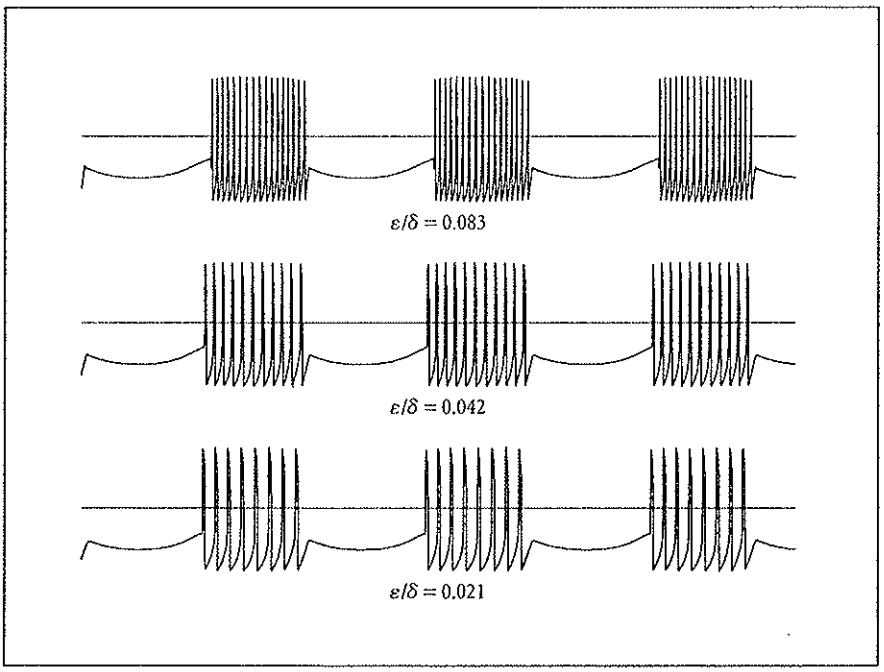

Fig. 4. Dependency of the number of spikes in terms of the ratio ε/δ.

so-called homoclinic orbit; a bifurcation takes place at this point, with a periodic orbit being born (or destroyed) in the process.

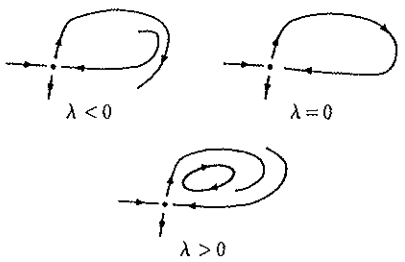

These three bifurcations – the saddle-node, Hopf and homoclinic bifurcations – represent a few of the typical topological transformations that one expects to find in low-dimensional dynamical systems; hence, it is natural to wonder if some combination of these bifurcations in interaction might generate bursting dynamics. Is there a simple scenario that fits the bill? Earlier models for bursting have invoked these three bifurcations in various combinations; here Doss-Bachelet et al. illustrate a simpler scenario involving the Hopf bifurcation only.

They consider the two-dimensional FitzHugh-Nagumo system of equations (eq. 2.1) – an archetypal set of nonlinear equations with rich behavior. To begin with, they first revisit the classical analysis of this system and show that it exhibits a Hopf bifurcation as one varies the parameter c. For the case $b = 0$, these equations have a single fixed point if c lies in a neighborhood of $c_0 = -2/\sqrt{3}$; but c_0 is a point of bifurcation, and the character of the flow changes here. For c slightly less than c_0 (or, equivalently, $\Delta < 0$, in equation 2.2), the fixed point is an attractive focus (all nearby points spiral in toward it); for c slightly larger than c_0 ($\Delta > 0$), the fixed point is a repulsive focus. As the fixed point loses stability, an attractive limit cycle emerges. So for c slightly larger than c_0, the system exhibits a repulsive focus located inside an attractive limit cycle.

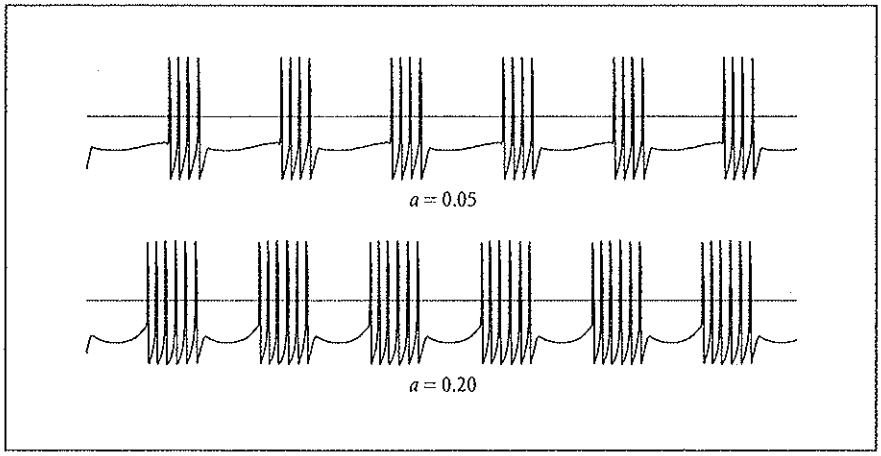

Fig. 5. Dependency of the number of spikes in terms of the parameter *a*.

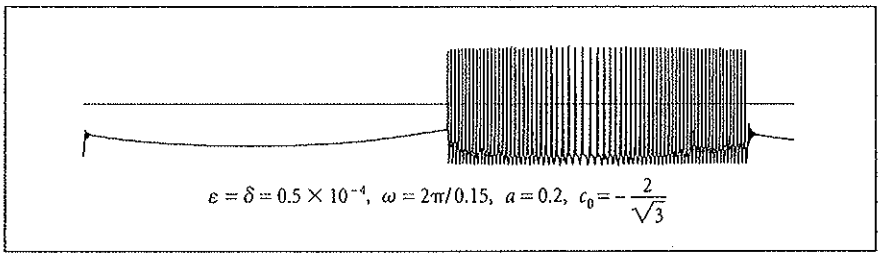

Fig. 6. A large number of spikes seen on the wave.

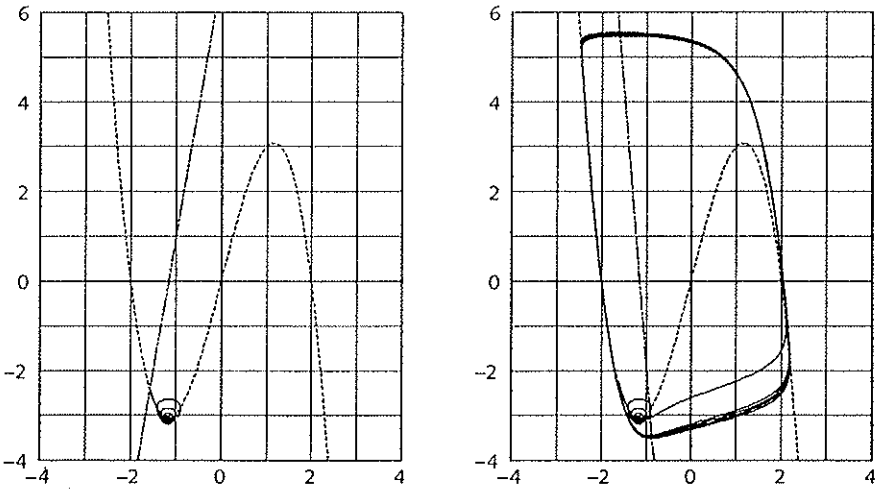

Fig. 7. The corresponding phase plane analysis.

This Hopf bifurcation provides a basic mechanism for bursting. Suppose that the parameter c is not merely a constant parameter, but fluctuates slowly in value as the result of some other dynamical process. If c drifts periodically above and below the critical value c_0, this would cause the dynamical system in equation 2.1 to pass repeatedly through the Hopf bifurcation, first in one direction and then in the other. During intervals with c less than c_0, the system trajectory would settle near the stable fixed point and remain there – the system would be in a quiescent state. Any movement of c above c_0 would drive the trajectory away from the now repulsive fixed point, and it would rapidly settle near the attracting limit cycle. Now the system would exhibit a period of oscillatory behavior, which would persist until c again fell below c_0. As long as the fluctuations in c are slow compared to the oscillations of the limit cycle, then bursting behavior like that seen in real biological systems would result.

The discussion in the paper is complicated somewhat by the parameters ε and δ, which are included so as to account for the possibility that the dynamics in one variable, x, may take place significantly faster than those of the other variable, y. This can be modeled by making the ratio ε/δ small, and in the limit in which $\varepsilon/\delta \rightarrow 0$ one needs the techniques of the so-called 'singular perturbation theory' to analyze the bifurcation. This technical aspect is not crucial to understanding the basic results of the paper, but the separation of timescales is important, for it helps to produce bursts that look like those seen in real biological systems.

The authors illustrate this in a variety of simulations. In fact, bursting dynamics can be produced not only with fluctuations in the parameter c in equation 2.1, but by controlling the parameter b instead. The authors show this with numerical simulations of their equation 3.1, and figures 3–6 show the results for various val-

References

1 Atwater I, Dawson CM, Scott A, Eddlestone G, Rojas E: The nature of the oscillatory behavior in electrical activity from pancreatic β-cell. Horm Metabol Res Suppl 1980;10:31–37.

2 Chay TR, Keizer J: Minimal model for membrane oscillations in the pancreatic β-cell. Biophys J 1983;42:181–190.

3 Rinzel J, Lee YS: Dissection of a model for neuronal parabolic bursting. J Math Biol 1989;25:653–675.

4 Rinzel J: A formal classification of bursting mechanisms in excitable systems; in Teramoto E, Yamaguti M (eds): Mathematical Topics in Population Biology, Morphogenesis and Neurosciences. Lecture Notes in Biomathematics. Berlin, Springer, 1987, vol 71, pp 267–281.

5 Wang XJ, Rinzel J: Oscillatory and bursting properties of neurons; in Arbib E (ed): Brain Theory and Neural Networks. Cambridge, MIT Press, 1995, pp 686–691.

6 Bertram R, Butte MJ, Kiemel T, Sherman A: Topological and Phenomenological classification of Bursting oscillations. Bull Math Biol 1995;57: 413–439.

7 Hoppensteadt FC, Izhikevich EM: Weakly Connected Neural Networks. New York, Springer, 1997.

8 Pernarowski M: Fast subsystem bifurcation in a slowly varying Liénard system exhibiting bursting. Siam J Appl Math 1994;54:814–832.

9 Dangelmayr G, Guckenheimer J: On a four parameter family of planar vector fields. Arch Rat Mech Anal 1987;97:321–352.

10 de Vries G: Multiple bifurcations in a polynomial model of bursting oscillations. J Nonlinear Sci 1998;8:281–316.

11 Guckenheimer J, Willms AR: Asymptotic analysis of subcritical Hopf-homoclinic bifurcation. Physica D 2000;139:195–216.

12 Braaksma B: Singular Hopf bifurcation in systems with fast and slow variables. J Nonlinear Sci 1998;8:457–490.

13 Kopell N, Ermentrout GB: Subcellular oscillations and bursting. Math Biosci 1986;78:265–291.

14 Alexander JC, Doedel EJ, Othmer HG: On the resonance structure in a forced excitable system. Siam J Appl Math 1990;50:1373–1418.

15 Holden L, Erneux T: Slow passage through a Hopf bifurcation: From oscillatory to steady state solutions. Siam J Appl Math 1993;53:1045–1058.

16 Hodgkin AL, Huxley AF: A quantitative description of membrane current and its application to conduction and excitation in nerve. J Physiol 1952; 117:500–544.

17 Keener J, Sneyd J: Mathematical Physiology. Berlin, Springer, 1998.

18 Goldbeter A: Biochemical Oscillations and Cellular Rhythms. Cambridge University Press, Cambridge, 1996.

19 Arvanitaki A: Recherches sur la réponse oscillatoire locale de l'axone géant isolé de 'Sepia'. Arch Int Physiol 1939;49:209–256.

20 Guttman R, Feldman L, Jakobsson E: Frequency entrainment of squid axon membrane. J Memb Biol 1980;56:9–18.

21 Holden AV: The response of excitable membrane models to a cyclic input. Biol Cybernetics 1976;21:1–7.

22 Chialvo DR, Jalife J: Non-linear dynamics of cardiac oscillation and impulse propagation. Nature 1987;330:749–752.

23 Arvanitaki A: Effects evoked in an axon by the activity of a contiguous one. J Neurophysiol 1942;5: 89–108.

24 Malle C, Madariaga A, Deschênes M: Morphology and electrophysical properties of reticularis thalami neurons in cat: In vivo study of a thalamic pacemaker. J Neurosci 1986;6:2134–2145.

25 Arnold VI: Lectures on bifurcation and versal families. Math Surveys 1972;27:119–184. In Russian.

26 Crawford JD: Introduction to bifurcation theory. Rev Mod Phys 1991;63:999–1037.

OBITUARY

We regret to inform you that Editorial Board member Professor Per Bak, London has deceased.

SIAM J. APPL. MATH.
Vol. 49, No. 1, pp. 55-71, February 1989

003

THE SLOW PASSAGE THROUGH A HOPF BIFURCATION: DELAY, MEMORY EFFECTS, AND RESONANCE*

S. M. BAER†, T. ERNEUX‡, AND J. RINZEL†

Abstract. This paper explores analytically and numerically, in the context of the FitzHugh-Nagumo model of nerve membrane excitability, an interesting phenomenon that has been described as a delay or memory effect. It can occur when a parameter passes slowly through a Hopf bifurcation point and the system's response changes from a slowly varying steady state to slowly varying oscillations. On quantitative observation it is found that the transition is realized when the parameter is considerably beyond the value predicted from a straightforward bifurcation analysis which neglects the dynamic aspect of the parameter variation. This delay and its dependence on the speed of the parameter variation are described.

The model involves several parameters and particular singular limits are investigated. One in particular is the slow passage through a low frequency Hopf bifurcation where the system's response changes from a slowly varying steady state to slowly varying relaxation oscillations. We find in this case the onset of oscillations exhibits an advance rather than a delay.

This paper shows that in general delays in the onset of oscillations may be expected but that small amplitude noise and periodic environmental perturbations of near resonant frequency may decrease the delay and destroy the memory effect. This paper suggests that both deterministic and stochastic approaches will be important for comparing theoretical and experimental results in systems where slow passage through a Hopf bifurcation is the underlying mechanism for the onset of oscillations.

Key words. delayed Hopf bifurcation transition, memory effect, resonance, FitzHugh-Nagumo equations, nerve accommodation

AMS(MOS) subject classifications. C34, 92

1. Introduction.

In mathematical studies of bifurcation, it is customary to assume that the bifurcation or control parameter is independent of time. However, in many experiments that are modeled mathematically as bifurcation problems, the bifurcation parameter varies naturally with time, or it is deliberately varied by the experimenter. Typically, this variation is slow or is forced to be slow.

The recent interest in the effects of slowly varying control parameters arises in physical, engineering, biological, and mathematical contexts. The physical interest arises from the fact that the results of long-time experiments may depend on parameters that are slowly varying. For example, catalytic activities in chemical reactors are slowly declining due to chemical erosion and are decreasing the reactor performance [1], [2]. The effects of slowly varying parameters are not always undesirable. They may also lead to smooth transitions at bifurcation points and mediate a gradual change in the system to a new mode of behavior beyond the bifurcation point. This idea has been studied for quite different problems such as thermal convection [3], [4], laser instabilities [5], [6], and developmental transitions in biology [7].

From a modeling point of view, we expect that a slow variation of the control parameter can be useful for the experimental or numerical determination of the bifurcation diagram of the stable solutions. Also, to understand certain complicated multi-scale dynamic phenomena [8], it is useful to study the bifurcation structure of the fast processes with the slow variables treated as slowly varying control parameters.

* Received by the editors June 3, 1987; accepted for publication November 13, 1987.

† Mathematical Research Branch, NIDDK, National Institutes of Health, Bethesda, Maryland 20892.

‡ Department of Engineeering Sciences and Applied Mathematics, Northwestern University, Evanston, Illinois 60208. This work was supported by the Air Force of Scientific Research under grant AFOSR85-0150 and the National Science Foundation under Grant DMS-8701302.

In such cases, it is important that we have detailed knowledge of the transition near the bifurcation point where transients are very slow.

From a mathematical point of view, these problems are formulated by non-autonomous differential equations that are difficult to solve. The study of these problems has led to new and interesting mathematical issues [9]–[11]. References [9]–[11] investigate the slow passage through a steady bifurcation or a steady limit point. An interesting study of the effects of a slowly varying parameter on a Hopf bifurcation is given for the slow passage through resonance [26], [27].

In this paper, we concentrate on the slow passage through a Hopf bifurcation. As we shall demonstrate, this case is quite different from a steady bifurcation or limit point. Our results for the Hopf bifurcation raise a series of new questions on the control of bifurcation instabilities. We shall consider a specific model problem for the Hopf bifurcation because our goal is to explore the effects of a slowly varying parameter both analytically and numerically. For example, one interesting phenomenon has been described as a delay or memory effect. It can occur when a parameter passes slowly through a Hopf bifurcation point and the system's response changes from a slowly varying steady state to slowly varying oscillations. On quantitative observations (see Fig. 1(a), (b)) we find that the transition is realized when the parameter is considerably beyond the value predicted from a straightforward bifurcation analysis which neglects the dynamic aspect of the parameter variation. We describe this delay and its dependence on the speed of the parameter variation. Also, we show that the delay is sensitive to small amplitude noise and to periodic environmental perturbations of near resonant frequency. This sensitivity may be helpful in the accurate determination of bifurcation points. The model involves several parameters and particular (singular) limits are investigated. These limits reveal other interesting features on the slow passage through the bifurcation point.

We employ the specific problem of the FitzHugh–Nagumo equations as a model to describe the mathematical and qualitative features of the slow passage through a Hopf bifurcation. Many of these features occur for other models [25].

2. Formulation.

2.1. The FitzHugh–Nagumo equations. In the early 1950s, Hodgkin and Huxley [12] proposed a model that describes the generation and propagation of the nerve impulse along the giant axon of the squid. The model consists of a four-variable system of nonlinear partial differential equations. Subsequently, Nagumo et al. [13] and FitzHugh [14] developed a simpler two-variable system, which describes the main qualitative features of the original Hodgkin–Huxley equations and which is analytically more tractable. The so-called FitzHugh–Nagumo (FHN) equations for the space clamped (i.e., spatially uniform) segment of axon have the form

$$\frac{dv}{dt} = -f(v) - w + I(t), \tag{2.1a}$$

$$\frac{dw}{dt} = b(v - \gamma w), \tag{2.1b}$$

where b and γ are positive constants and $f(v)$ is a cubic-shaped function given by

$$f(v) = v(v-a)(v-1), \qquad 0 < a < \tfrac{1}{2}. \tag{2.1c}$$

Here $v(t)$ denotes the potential difference at time t across the membrane of the axon and w represents a recovery current which, according to the second equation (2.1b), responds slowly, when b is small, to changes in v. The first equation (2.1a) expresses

Kirchhoff's current law as applied to the membrane; the capacitive, recovery, and instantaneous nonlinear currents sum to equal the applied current, $I(t)$. The applied current is our control or bifurcation parameter. In this section, we consider either constant intensities or slowly varying intensities of the form

$$I(\varepsilon t) = I_i + \varepsilon t, \qquad 0 < \varepsilon \ll 1. \tag{2.1d}$$

From biophysical considerations, it is reasonable to restrict γ so that

$$\gamma < 3(1 - a + a^2)^{-1}. \tag{2.2}$$

This insures that (2.1) with $\varepsilon = 0$ have a unique steady state. The steady state $(v, w) = (v_s(I), w_s(I))$ satisfies the conditions

$$w_s = v_s/\gamma, \qquad I = f(v_s) + v_s/\gamma. \tag{2.3}$$

To analyze its stability, we consider small perturbations of the form $v = v_s + p\,e^{\lambda t}$ and $w = w_s + q\,e^{\lambda t}$ where $|p| \ll 1$ and $|q| \ll 1$. This leads to the following characteristic equation for λ

$$\lambda^2 + A\lambda + B = 0 \tag{2.4a}$$

where

$$A = f'(v_s(I)) + b\gamma, \tag{2.4b}$$

$$B = b[1 + \gamma f'(v_s(I))] \tag{2.4c}$$

The steady state is stable (unstable) if $A > 0$, $B > 0$ ($A < 0$ and/or $B < 0$). From the conditions $A = 0$, $B > 0$ we find two Hopf bifurcation points $I = I_\pm$. They satisfy the conditions

$$v_s(I_\pm) = v_\pm = \tfrac{1}{3}[a + 1 \pm (a^2 + 1 - a - 3b\gamma)^{1/2}] \tag{2.5}$$

$$\omega_0^2 = b(1 - b\gamma^2) > 0. \tag{2.6}$$

When $I < I_-$ or $I > I_+$ ($I_- < I < I_+$), the steady state is stable (unstable). To analyze the response of the system near I_- or I_+, the approach of bifurcation theory is particularly useful. When $I > I_-$ or $I < I_+$, the transition to the oscillations can be smooth (supercritical bifurcation) or hard (subcritical bifurcation). Details of the bifurcation analysis are given in [15]-[17].

2.2. Response to the slowly varying parameter. We now consider the effect of a slowly varying parameter. We assume that the system is initially at a stable steady state i.e., $I_i < I_-$. Figure 1 illustrates the response to the slow, linearly rising current (2.1d); in Fig. 1(a), v is plotted versus t and in Fig. 1(b), v is plotted versus I. For these parameter values, the Hopf bifurcation at I_- is supercritical. From the bifurcation structure (Fig. 1(b)), one might expect that the response would approximately track the slowly varying steady state $(v, w) = (v_s(I), w_s(I))$, and then, as I increases through I_-, the response would switch to the large amplitude oscillations. Such a switch is seen, but the value $I = I_j$ at which it occurs is considerably delayed beyond I_-. Moreover, the amount of delay increases with distance that I_i is from I_- (Fig. 1(c)). To understand this delay, we execute the following strategy: first, we determine a new (slowly varying) basic reference solution as a perturbation of the steady state $(v, w) = (v_s(I), w_s(I))$. Then, we analyze its stability with respect to the fast time of the oscillations. We show that loss in stability occurs well beyond I_-.

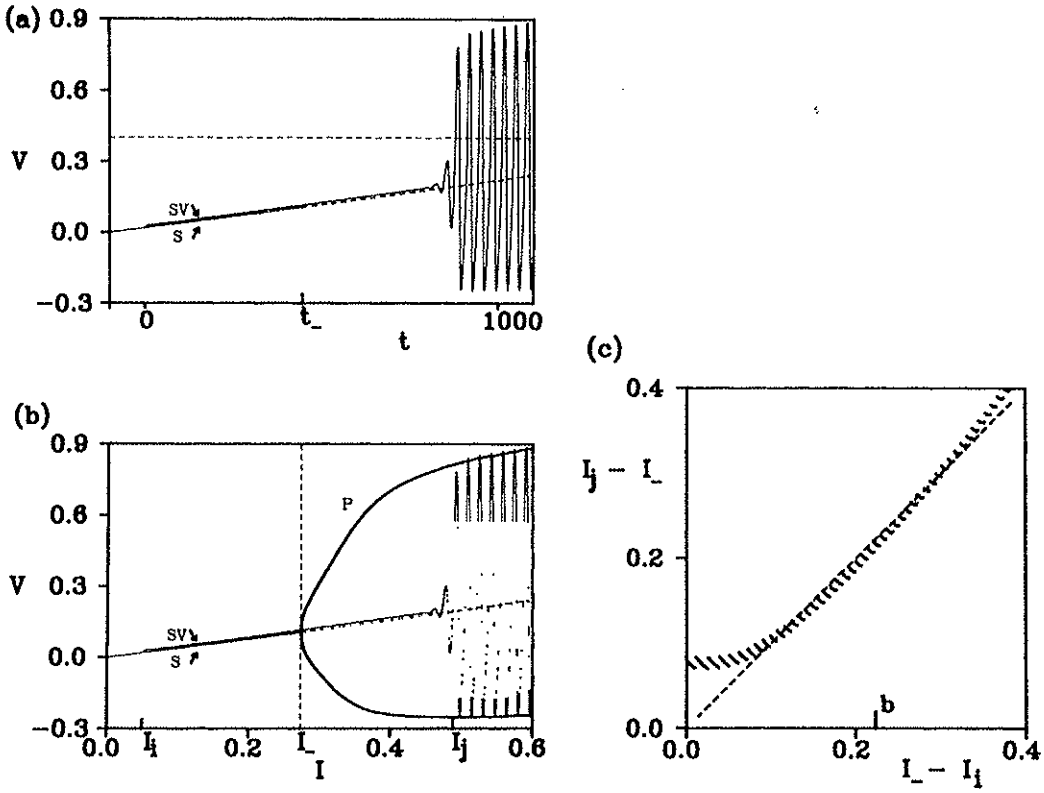

FIG. 1. *Delay or memory effect.* (a) *The transition to slowly varying oscillations is computed from the numerical integration of* (2.1) *for current* $I(\varepsilon t) = I_i + \varepsilon t$, *where* $I_i = 0.05$. *Trajectory* (*SV*) *shows that the membrane potential varies slowly in response to a slowly rising current. The onset of oscillations is indicated when the trajectory first crosses the horizontal dashed line* $v = 0.4$, *at* $t = 880$. *Curve* (*S*) *is the steady state solution to* (2.1) *for increasing* (*time-independent*) *values of I. Solid denotes stable and dashed denotes unstable steady state solutions. A stability change occurs at the Hopf bifurcation point* $I_- = 0.273$, *which corresponds to time* $t_- = (I_- - I_i)/\varepsilon = 446$. *Compared to the time of stability loss estimated from the Hopf bifurcation analysis, the onset of oscillations is considerably delayed.* (b) *The slowly varying response* (*SV*) *for slowly increasing I; and the steady state solution* (*S*) *and bifurcating branch of periodic solutions* (*P*) *for the parametric dependence on I. The onset of oscillations occurs at* $I_j = 0.490$, *well past the value* $I_- = 0.273$ *predicted from a Hopf bifurcation analysis, however, the amplitude of oscillations continue to track the bifurcation envelope computed using* AUTO [19]. (c) *Numerical determination of* I_j *for many values of* I_i. *Label b refers to cases* (a) *and* (b) *above. The delay increases as* $(I_- - I_i)$ *increases. Superimposed* (*dashed*) *are the predicted values of* I_j, *from the numerical integration of* (3.5), *at which the slowly varying solution loses stability with respect to the fast time. This illustrates the memory effect. Parameter values are* $a = 0.2$, $b = 0.05$, $\gamma = 0.4$, *and* $\varepsilon = 5 \times 10^{-4}$.

The "slowly varying steady state" is found by determining a solution of (2.1) of the form

$$\bar{v}(\tau, \varepsilon) = \sum_{j=0}^{\infty} \varepsilon^j v_j(\tau), \qquad \bar{w}(\tau, \varepsilon) = \sum_{j=0}^{\infty} \varepsilon^j w_j(\tau) \tag{2.7}$$

where τ is a slow time variable defined by

$$\tau = \varepsilon t. \tag{2.8}$$

The coefficients $v_j(\tau)$ and $w_j(\tau)$ are obtained by inserting (2.7) and (2.8) into (2.1) and equating to zero the coefficients of each power of ε. The analysis of the first two

problems leads to the following results:

$$\bar{v}(\tau, \varepsilon) = v_s(I(\tau)) + \varepsilon \frac{\omega_0^2}{b\gamma B} v_s'(\tau) + O(\varepsilon^2) \tag{2.9}$$

and

$$\bar{w}(\tau, \varepsilon) = w_s(I(\tau)) - \varepsilon \frac{A}{B\gamma} v_s'(\tau) + O(\varepsilon^2) \tag{2.10}$$

where $v_s' = dv_s/d\tau$ and A, B and ω_0^2 are defined by (2.4b), (2.4c), and (2.6), respectively. From (2.9) and (2.10), we note that the expansion of the slowly varying solution does not become singular at the Hopf bifurcation point $I = I_-$. Indeed at $I = I_-$, $B = \omega_0^2 \neq 0$ and the functions in (2.9) and (2.10) remain $O(1)$ quantities. This contrasts with the case of a steady bifurcation or limit point where the expansion of the slowly varying solution becomes singular at and near the bifurcation or limit point [1], [10]. Note however from (2.9) and using the definitions (2.4) and (2.6) that the expansion is nonuniform if $b = O(\varepsilon)$ or $\gamma = O(\varepsilon)$. Both cases are of practical interest and we consider them in §§ 4 and 5, respectively.

Numerical computations were performed on a Vax 8600 using a classical fourth-order Runge-Kutta method with fixed step size ($DT = 0.1$). Results were also computed using a Gear method [18] for stiff differential equations. The two methods showed excellent agreement. To retain accuracy using Gear's method in problems with slow passage through bifurcation points, a tight control of relative error is imperative (we used TOL $= 10^{-12}$). Hence we found the RK4 method to be more efficient for these calculations. In addition, the simplicity of the method makes our results easily reproducible. When a control parameter varies slowly and/or when $I_- - I_i$ is large, numerical solutions to (2.1) are particularly sensitive to roundoff error. Thus we were careful to compare computations in single, double, and quadruple precision. The results for all figures (except as noted in Figs. 1(c) and 4) were computed in double precision. In numerical calculations the onset of oscillations was defined as the time t_j when the v versus t trajectory first crossed the value $v = 0.4$. The bifurcation diagram in Fig. 1(b) was computed using AUTO [19].

3. Stability of the slowly varying solution. In this section, we analyze the stability of the slowly varying solution $(v, w) = (\bar{v}, \bar{w})$. After introducing the deviations

$$\begin{aligned} V(t, \varepsilon) &= v(t, \varepsilon) - \bar{v}(\tau, \varepsilon), \\ W(t, \varepsilon) &= w(t, \varepsilon) - \bar{w}(\tau, \varepsilon) \end{aligned} \tag{3.1}$$

into (2.1), we obtain the following linearized equations for V and W:

$$\begin{aligned} \frac{dV}{dt} &= -f'(\bar{v}(\tau, \varepsilon))\, V - W \\ \frac{dW}{dt} &= b(V - \gamma W). \end{aligned} \tag{3.2}$$

Assuming now zero initial conditions for V and W, we solve (3.2) by a WKB method [24]. Specifically, we seek a solution of (3.2) of the form

$$\begin{aligned} V(t, \varepsilon) &= V(\tau, \varepsilon) = \exp[\sigma(\tau)/\varepsilon] \sum_{j=0}^{\infty} \varepsilon^j V_j(\tau), \\ W(t, \varepsilon) &= W(\tau, \varepsilon) = \exp[\sigma(\tau)/\varepsilon] \sum_{j=0}^{\infty} \varepsilon^j W_j(\tau). \end{aligned} \tag{3.3}$$

Introducing (3.3) into (3.2) and equating to zero the coefficients of each power of ε, we obtain the following problem for V_0 and W_0:

$$\begin{aligned} \sigma'(\tau)V_0 &= -f'(v_s(\tau))V_0 - W_0, \\ \sigma'(\tau)W_0 &= b(V_0 - \gamma W_0). \end{aligned} \tag{3.4}$$

A nontrivial solution is possible only if $\lambda = \sigma'(\tau)$ satisfies the characteristic equation (2.4a) where the coefficients A and B are now functions of $I(\tau)$. From (3.3) we conclude that at the time τ, the slowly varying solution is stable with respect to the fast time t if

$$\mathrm{Re}\,(\sigma) = \int_0^\tau \mathrm{Re}\,[\lambda(s)]\,ds < 0. \tag{3.5}$$

When the quantity $\mathrm{Re}\,(\sigma)$ becomes positive then the solution (3.3) exhibits rapid exponential growth and the slowly varying solution is therefore unstable on the fast time scale. From (3.5) we conclude that there is a memory effect. Destabilization of the slowly varying solution does not occur immediately when $\mathrm{Re}\,[\lambda(s)]$ changes sign (i.e., when I increases through I_-), but only after the integrated effect of $\mathrm{Re}\,(\lambda) > 0$ overcomes the accumulated influence of $\mathrm{Re}\,(\lambda) < 0$. Moreover, (3.5) is independent of ε so that the delay persists even if the control parameter is tuned infinitesimally slowly. The importance of this integral condition for predicting the delay was seen previously for steady bifurcation problems [5], [10] and for bursting oscillations [8].

We remark that the series (3.3) represents a valid approximation on the time interval τ if the discriminant of (2.4a) given by

$$D(\tau) = A^2(I(\tau)) - 4B(I(\tau)) \tag{3.6}$$

does not vanish. Points where $D(\tau)$ vanishes are where (v_s, w_s) changes from a node to a focus. These points are called turning points (not to be confused with limit points). If $I_- - I_i$ is not sufficiently small, $D(\tau)$ may change sign on the interval of interest and the WKB solution (3.3) becomes invalid in the neighborhood of the turning points. Nevertheless, a global approximation to the solution of (3.2) can be obtained by the method of matched asymptotic expansions. In this study, we consider only the simplest case where there are no turning points, i.e., $D(\tau) < 0$ during the time interval of interest. The case with turning points will be presented elsewhere. Its analysis leads to a stability condition similar to (3.5).

We have obtained explicit expressions for the delay and for conditions which guarantee that $D(\tau)$ remains negative by exploiting algebraic simplifications which arise in the parameter range $O < a \ll 1$. In the limit $a \to 0$, we assume $I(\tau) = O(a)$, and find from (2.3) and then from (2.4(b), (c)) the following expressions for v_s, A, and B:

$$v_s(I) = \gamma I + O(a^2), \tag{3.7}$$

$$A = -2\gamma(I - I_-^0) + O(a^2), \tag{3.8}$$

$$B = b + O(a^2 b) \tag{3.9}$$

where $I_-^0 = a/2\gamma$ corresponds to the leading approximation of the first Hopf bifurcation point $I = I_-$ (from (2.5), $v_- = a/2 + O(a^2)$ and then using (2.3), $I_- = I_-^0 + O(a^2)$). Using the definition (3.6), we obtain an approximate expression for $D(\tau)$

$$D(\tau) \cong 4\gamma^2(I(\tau) - I_-^0)^2 - 4b \tag{3.10}$$

or, equivalently,

$$D(\tau) \cong 4\gamma^2(I - I_-^0 - b^{1/2}/\gamma)(I - I_-^0 + b^{1/2}/\gamma). \tag{3.11}$$

At $I = I_-^0$, $D(\tau) < 0$ and remains negative provided that

$$I_-^0 - b^{1/2}/\gamma < I(\tau) < I_-^0 + b^{1/2}/\gamma. \tag{3.12}$$

Thus, if $I_i > I_-^0 - b^{1/2}/\gamma$, then $D(\tau)$ is negative until $I = I_-^0 + b^{1/2}\gamma$ is reached. Because we assume that $D(\tau) < 0$ during the time interval of interest, the stability change of the slowly varying solution appears at $\tau = \tau_j$, which is defined by the condition

$$\int_0^{\tau_j} \mathrm{Re}\,[\lambda(s)]\, ds = 0 \tag{3.13a}$$

or, equivalently,

$$\int_0^{\tau_j} A(s)\, ds \equiv -2\gamma \int_0^{\tau_j} (I(s) - I_-^0)\, ds = -\gamma\tau_j [(I(\tau_j) - I_-^0) - (I_-^0 - I_i)] = 0. \tag{3.13b}$$

Thus, since, $I_- = I_-^0 + O(a^2)$, we conclude from (3.13b) that

$$I(\tau_j) - I_- = I_- - I_i \tag{3.14}$$

to lowest order. Using (3.14) we easily verify that $D(\tau) < 0$ for $0 \leqq \tau \leqq \tau_j$. We call $I(\tau_j) - I_-$ the delay of the bifurcation transition. The expression (3.14) emphasizes two important features of the slow passage through the Hopf bifurcation: first, it is independent of ε, the rate of change of the control parameter I; second, the stability change of the slowly varying reference solution appears at a distance that is $O(1)$, with respect to ε, from the static bifurcation point I_-, as seen in Fig. 1. This distance can be controlled by changing I_i, the initial value of I. We thus observe a memory effect.

In Fig. 1(c), we illustrate the memory effect by integrating (2.1) numerically. Our calculations confirm that increasing $I_- - I_i$ increases the delay of the bifurcation transition. Moreover, (3.14) is in excellent agreement with the numerical results when $I_- - I_i > 0.2$. For $I_- - I_i < 0.2$ the numerics apparently deviate from our analytic prediction. This is due to the bifurcation being supercritical. The bifurcating branch of periodic solutions is locally stable, so when I_i is near the static Hopf point there are several small oscillations whose amplitude remain below the prescribed "threshold." For larger delays there is usually only one or two such oscillations. Another feature observed in Fig. 1(c) is a sawtooth jump pattern that occurs because the final subthreshold oscillation before onset shifts in phase as $I_- - I_i$ increases. Eventually a value is reached that delays the onset for one more subthreshold oscillation. The size of the jump ΔI_j is estimated by multiplying the ramp speed ε by the period of the oscillation $2\pi/\omega_0$, that is $\Delta I_j = \varepsilon(2\pi/\omega_0)$. When $I_- - I_i = 0$, six subthreshold oscillations occur before onset. Thus the jump magnitude in this case is about $6\varepsilon(2\pi/\omega_0)$.

4. Slow passage through a low frequency Hopf bifurcation. We now investigate the dynamics of the case b small, which appeared as a singularity of the slowly varying reference solution (2.9) and (2.10). A detailed study of this singularity ($\varepsilon = O(b)$) leads to a rich discussion and will be presented elsewhere. In this section, we consider a particular relation between ε, $I_i - I_-$, and b that is motivated by the parameter values used in our numerical study of the FHN equations ($\varepsilon = O(b^{3/2})$ and $I_i - I_- = O(b^{1/2})$). This special relation between the parameters does not correspond to the singularity of the slowly varying solution. However, it can be shown that the Hopf bifurcation is singular in this critical regime [20]. This motivates a careful analysis of this case. To lowest order, we find that the dynamical description is given by a nonlinear problem. Although we do not solve it analytically, we obtain useful insight showing that in this case the onset of oscillations exhibits an advance rather than a delay.